Hydrogen-bonding interactions in acetic acid monohydrates and dihydrates by density-functional theory calculations

Q. Gao and K. T. Leung[a)]
Department of Chemistry, University of Waterloo, Waterloo, Ontario N2L 3G1, Canada

(Received 29 March 2005; accepted 29 June 2005; published online 25 August 2005)

Equilibrium structures and the respective binding energies of acetic acid monohydrates and dihydrates have been determined by density-functional theory calculations with different basis sets, including 6-31+G($3d,p$), 6-311++G(d,p), and 6-311++G($3df,3pd$). Given that the C═O and OH groups in acetic acid provide the predominant hydrogen-bonding interactions with water, six stable conformer structures have been found each for the monohydrate and *syn*-dihydrate. Of the three *syn*- and three *anti*-conformers of acetic acid with water, the most stable monohydrate structure is found to be that of the *syn*-conformer bonding with water in a cyclic double H-bonded geometry. Similarly, the *syn*-conformer bonding with two water molecules in a cyclic double H-bonded geometry has also been determined to be the most stable among the six plausible structures for the *syn*-dihydrate. Frequency analysis of the stable conformers has been performed and the vibrational spectra of the most stable monohydrate and dihydrate structures are compared with the experimental gas-phase and matrix data. Furthermore, the calculated binding energies between an acetic acid and a water molecule for both monohydrate and dihydrate are larger than that between two water molecules, which supports our recent experimental observation of coevaporation of acetic acid with water upon annealing acetic acid on ice. © *2005 American Institute of Physics*. [DOI: 10.1063/1.2006089]

I. INTRODUCTION

The investigation of water complexes has attracted much recent attention because of the fundamental interest in the molecular interactions of clathrate hydrates, aqueous solutions, and adsorbates on ice.[1] Since the intermolecular interactions in these weakly bound systems are complex and largely pair additive, the use of model systems calculated by *ab initio* methods could provide considerable insights into these interactions and aid the interpretation of our experimental data. Unlike traditional semiempirical methods, *ab initio* calculations can also be used to provide not just structural and energy properties but also vibrational analysis without the use of empirical force fields,[2–4] which have become quite useful for the assignment and interpretation of infrared and Raman spectra as well as for the determination of molecular structures and potential-energy surfaces.[5] Although the Hartree-Fock (HF) method generally overestimates vibrational frequencies by approximately 10% due to the neglect of electron correlation and anharmonicity effect,[6] this method has remained to be one of the most useful and relatively inexpensive techniques for vibrational analysis. With ten monolayers of water molecules interchanging between the solid and vapor phases per second at 180 K,[7,8] the ice surface provides a highly dynamical medium for various fundamental surface processes. In particular, the diffusion and desorption of water molecules at 180 K occur on time scales of 5 and 90 ms, respectively,[9] while the adsorption of a guest molecule typically occurs on a picosecond time scale.[10] Due to the large difference in the time scales, the ice surface would appear static to an incoming guest molecule, therefore validating the use of equilibrium structures as obtained from *ab initio* calculations to model these intricate surface phenomena.

Ab initio HF methods at the 6-31G** level have often been used to provide reasonable estimates of the energies of both conformational changes and hydrogen bonding of fairly large systems where more sophisticated calculations are not feasible.[11] It is well known, however, that a more reliable description of these weak interactions generally requires consideration of electron correlation not included in the HF method.[6] On the other hand, density–functional theory (DFT) involving, in particular, the B3LYP hybrid functional[12–14] has proven to be useful in this regard especially for H-bonded complexes.[15–17] DFT offers an electron correlation correction of similar or superior quality to second-order Møller-Plesset perturbation theory[18–20] (MP2) but at a considerably lower computational cost. The cost advantage becomes progressively greater with an increasing size of the system where geometry optimization is time consuming. DFT calculations using a very large diffuse basis set such as 6-311++G($3df,3pd$) should also provide reliable H-bonding interaction energies for weakly bound systems.[21] While the smaller basis sets (e.g., 6-31G**) may not yield adequate results, this type of a very large basis set is unfortunately found to be impractical and cost prohibitive for large systems (e.g., over ten-water molecules). Consequently, the smaller nonstandard diffuse polarization basis sets [e.g., 6-31+G($3d,p$) used in the present work] developed by Ochterski could be a good compromise in achieving the desired accu-

a)Electronic mail: tong@uwaterloo.ca

racy at a moderate computing cost for H-bonded systems such as water.[21,22] Since hydrogen bonds are largely electrostatic in nature, the accuracy of the molecular dipole moment would provide a measure of the quality of the calculation for hydrogen-bonding interaction. For example, the HF method overestimates the experimental dipole moment of water (1.854 D) and acetic acid (1.74 D) by 15.8% and 5.1%, respectively, with the 6-31G** basis set. On the other hand, the DFT method, which partially includes electron correlation, overestimates the dipole moment by 10.2% and 7.7% for water and acetic acid, respectively, with the same 6-31G** basis set. With the larger 6-31+G($3d,p$) [6-311++G($3df,3pd$)] basis set, the DFT calculation only overestimates the experimental values by 1.7% (1.9%) and 2.8% (2.4%) for water and acetic acid, respectively.

The interactions of acetic acid with water are particularly interesting due to the presence of the carbonyl and hydroxyl groups in the carboxylic acid group, which could provide hydrogen-bonding interactions, respectively, with the dangling H and dangling O atoms of the water molecules. Furthermore, the carbonyl and hydroxyl groups in acetic acid could also facilitate dimer and oligomer formations expected in the solid phase. Recently, we studied the interactions of acetic acid solids and of acetic acid adsorbed on ultrathin noncrystalline and polycrystalline ice films by Fourier transform infrared (FTIR) reflection-absorption spectroscopy (RAS).[23] We now provide an *ab initio* computational study in order to aid our spectral assignments and infer the nature of the molecular interactions that underline the adsorption and thermal evolution. In particular, equilibrium structures and binding energies of acetic acid monohydrates and dihydrates have been obtained by DFT calculations with sizable basis sets. The effects due to the size of the basis set and the basis set superposition errors have been investigated, while vibrational analysis has been performed to follow the shifts in new intermolecular and intramolecular frequencies as a result of the complex formation.

II. COMPUTATIONAL DETAILS

All the calculations have been performed using the GAUSSIAN98 suite of programs[24] at a homebuilt computer cluster based on the Pentium-4 technology. The total electronic energies, equilibrium geometries, and corresponding harmonic vibrational frequencies of possible conformations of the acetic acid monohydrate and dihydrate have been determined by using the DFT method at the Becke's three-parameter hybrid functional[12,13] with the Lee-Yang-Parr correlation functional[14] (B3LYP) level. Restricted HF calculations with the 6-31G** basis set have been used to provide the initial structures for the subsequent DFT calculations involving larger basis sets, including 6-31+G($3d,p$), 6-311++G(d,p), and 6 311++G($3df,3pd$). Zero-point vibrational energy (E_{ZP}) corrections have been obtained in the calculations but not included in the calculated total energies and relative stabilities as well as the binding energies reported in the present work. The binding energies ΔE [$=E_{\text{hydrate}}-(E_{\text{acetic acid}}+n\,E_{\text{water}})$] for the monohydrate ($n=1$) and dihydrate ($n=2$) have also been determined without the function counterpoise corrections for the basis set superposition error (BSSE),[25,26] where the E's correspond to the total energies of the hydrate, acetic acid, and water. For a molecular system involving two subsystems A and B (as in the monohydrate case), the E_{BSSE} is given by

$$E_{\text{BSSE}} = E_A(A) - E_A(AB) + E_B(B) - E_B(AB),$$

where $E_X(Y)$ is the total energy of subsystem X obtained with the basis set of Y in the equilibrium geometry of the entire system. For a system with three subsystems A, B, and C (as in the dihydrate case), the corresponding E_{BSSE} is given by[27]

$$\begin{aligned} E_{\text{BSSE}} = &- E_{AB}(ABC) + E_{AB}(AB) - E_{AC}(ABC) + E_{AC}(AC) \\ &- E_{BC}(ABC) + E_{BC}(BC) - E_A(AB) - E_A(AC) \\ &+ E_A(ABC) + E_A(A) - E_B(AB) - E_B(BC) \\ &+ E_B(ABC) + E_B(B) - E_C(AC) - E_C(BC) \\ &+ E_C(ABC) + E_C(C). \end{aligned}$$

In general, the magnitude of E_{BSSE} decreases with an increasing size of the basis set, especially when diffuse and polarization functions are included in the B3LYP method.[28] For larger basis sets, the inclusion of E_{BSSE} correction therefore has minor effects on the binding energy ΔE. The function counterpoise method only provides an upper limit to the true basis set superposition error, and the "true" binding energy is expected to be between ΔE and $\Delta E+E_{\text{BSSE}}$.

There are two conformers for the acetic acid molecule: the *syn*- and *anti*-conformers with their respective hydroxyl H pointing, respectively, along and opposite to the direction of the carbonyl O. The *syn*-conformer is also found to be more stable than the *anti*-conformer by 28.9 kJ mol^{-1} (with a rotational barrier of 55.2 kJ mol^{-1}) in a reference interaction site model-self-consistent field (RISM-SCF)/multiconfigurational self-consistent field (MCSCF) calculation reported by Sato and Hirata[29] and by 21.4 kJ mol^{-1} in the present DFT/6-311++G($3df,3pd$) calculation by us. The corresponding Boltzmann population distribution favors the *syn*- over the *anti*-conformer by 25 000 to 1 at room temperature. In Table I, we compare the equilibrium structures and the corresponding dipole moments and total energies for the *syn*- and *anti*-conformers of acetic acid and for a water molecule obtained by different *ab initio* calculations with the available experimental data.[30] Evidently, all of our calculations show the same relative stability between the *syn*- and *anti*-conformers of acetic acid. It is also not surprising that relative to the B3LYP calculations with larger basis sets [6-31+G($3d,p$), 6-311++G(d,p), and 6-311++G($3df,3pd$)], both the HF and B3LYP calculations with the 6-31G** basis set generally give a poorer agreement with the experimental values for the dipole moment and the structural parameters [e.g., R(O–H)]. Furthermore, the larger the basis set (except for the nonstandard 6-31+G($3d,p$) basis set], the more negative is the total energy, as generally expected from the variational principle. However, the basis sets with more diffuse and polarization functions are expected to provide a more accurate description of the weakly bonded systems such as the H-bonded hydrates. We therefore concentrate our discussion below on the calculated results ob-

TABLE I. Comparison of the bond lengths R (Å), bond angles $\theta(^\circ)$, dipole moments μ, and total energies E without the zero-point vibrational energy E_{ZP} corrections (hartree) of the optimized equilibrium structures of *syn*- and *anti*-acetic acid and water with the experimental data.

	Geometrical parameters and properties[a]	HF/ 6-31G**	DFT/ 6-31G**	DFT/ 6-31+G(3*d*,*p*)	DFT/ 6-311++G (*d*,*p*)	DFT/ 6-311++G (3*df*,3*pd*)	Experimental values[b]
Syn- acetic acid	*R*(C–C)	1.501 2	1.507 4	1.505 2	1.504 5	1.502 5	1.520
	R(C–O)	1.330 9	1.357 4	1.358 2	1.358 3	1.354 9	1.364
	R(C=O)	1.187 2	1.210 5	1.207 9	1.204 9	1.202 2	1.214
	R(O–H)	0.948 1	0.972 4	0.971 3	0.969 1	0.967 9	0.97
	R(C–H)	1.079 4	1.089 0	1.089 1	1.087 5	1.084 6	1.102
	R′(C–H)	1.084 0	1.093 9	1.094 0	1.092 4	1.089 8	···
	θ(C–C–O)	111.94	111.43	111.74	111.49	111.60	110.6
	θ(C–C=O)	125.72	126.09	125.98	126.19	126.06	126.6
	θ(O=C–O)	122.34	122.49	122.27	122.32	122.34	122.8
	θ(C–O–H)	108.30	105.82	106.62	107.12	107.04	107.0
	μ(debye)	1.829 6	1.606 0	1.789 1	1.736 1	1.781 5	1.74
	E(hartree)	−227.822 171 43	−229.091 479 32	−229.118 586 70	−229.164 827 69	−229.181 571 20	
	E_{ZP}	0.066 72	0.062 00	0.061 55	0.061 49	0.061 56	
Antiacetic acid	*R*(C–C)	1.510 1	1.518 6	1.514 6	1.515 7	1.511 7	
	R(C–O)	1.336 6	1.363 8	1.365 3	1.365 3	1.361 4	
	R(C=O)	1.180 8	1.203 5	1.200 6	1.197 3	1.195 4	
	R(O–H)	0.943 4	0.967 7	0.966 6	0.964 6	0.963 4	
	R(C–H)	1.079 0	1.089 0	1.086 4	1.087 7	1.084 8	
	R′(C–H)	1.086 0	1.095 7	1.095 6	1.094 1	1.091 3	
	θ(C–C–O)	115.32	115.28	115.49	115.31	115.32	
	θ(C–C=O)	124.22	124.73	124.87	124.94	124.91	
	θ(O=C–O)	120.46	119.99	119.64	119.75	119.77	
	θ(C–O–H)	112.40	110.26	110.69	110.76	110.95	
	μ(debye)	4.737 6	4.289 0	4.411 6	4.5774	4.407 7	
	E(hartree)	−227.810 822 14	−229.081 690 06	−229.110 245 86	−229.155 390 94	−229.173 409 22	
	E_{ZP}	0.066 39	0.061 64	0.061 34	0.061 07	0.06134	
Water	*R*(O–H)	0.9432	0.965 2	0.964 2	0.962 0	0.961 0	0.958
	θ(H–O–H)	105.92	103.74	104.81	105.06	105.05	104.6
	μ(debye)	2.148 0	2.042 9	1.885 0	2.159 1	1.889 5	1.854
	E(hartree)	−76.023 614 93	−76.419 736 62	−76.440 552 17	−76.458 530 77	−76.464 511 50	
	E_{ZP}	0.023 19	0.021 37	0.021 33	0.021 29	0.021 32	

[a]The two C–H bond lengths for the methyl group in acetic acid are listed as *R* and *R′*.
[b]Reference 30.

tained by using the larger basis sets [6-31+G(3*d*,*p*), 6-311++G(*d*,*p*), and 6-311+G(3*df*,3*pd*)].

In the present work, we label the monohydrate and dihydrates of acetic acid as follows. For the conformers of the acetic acid monohydrate, the calculated equilibrium structures are identified by an uppercase letter S for the *syn*- and A for the *anti*-conformers of the acetic acid molecule, followed by a number indicating the relative position of the water molecule with respect to the acetic acid, with 1 for the carboxylic acid side, 2 for the methyl-carbonyl side, and 3 for the methyl-hydroxyl side. In the case of the dihydrate structures, an additional number is used to identify the relative position of the second water molecule following the same convention as the monohydrate.

III. RESULTS AND DISCUSSION

A. Conformers of acetic acid monohydrate

The equilibrium structures for the six conformers of the acetic acid monohydrate have been determined by DFT-B3LYP calculations with the nonstandard 6-31+G(3*d*,*p*), and the standard 6-311++G(*d*,*p*) and 6-311++G(3*df*,3*pd*) basis sets, with 185, 152, and 303 basis functions, respectively. Selected structural parameters along with the dipole moment, the total energy without the E_{ZP} correction, and the binding energy without the corresponding E_{BSSE} correction obtained by these calculations are presented in Table II. Evidently, the structural parameters and the energies obtained for all the basis sets are very similar to one another for all of the conformers. As expected, the larger the standard basis set, the lower is the calculated total energy. The conformer structures obtained by the largest basis set, 6-311++G(3*df*,3*pd*), exhibit the lowest total energies, and these structures are shown in Fig. 1. It should be noted that only minor changes (less than 2%) in the original structures of acetic acid and water molecules (Table I) are observed upon hydrate formation, for all calculations depicted in Table II. In particular, the C–O bond length in acetic acid is found to be slightly shortened concomitantly with a minor increase

TABLE II. Comparison of the bond lengths R(Å), bond angles θ(°), dipole moments μ, total energies E without the zero-point vibrational energy E_{ZP} corrections, and binding energies ΔE without the basis set superposition error E_{BSSE} corrections of the optimized equilibrium structures of acetic acid monohydrate conformers obtained by different calculations.

	Properties	DFT/ 6−31+G(3d,p)	DFT/ 6−311++G(d,p)	DFT/ 6−311++G(3df,3pd)
S1	$R(H_{OH}\cdots O_{H_2O})$, $\theta(OH\cdots O_{H_2O})$	1.8002,157.48	1.8062,156.40	1.8068,157.11
	$R(O_{CO}\cdots H_{H_2O})$, $\theta(O_{CO}\cdots HO_{H_2O})$	1.9522,140.26	1.9893,135.56	1.9600,139.82
	μ(debye)	1.4804	1.2539	1.3763
	$E(E_{ZP})$(hartree)	−305.574 490 77 (0.086 73)	−305.639 739 94 (0.08669)	−305.661 295 39 (0.08678)
	$\Delta E(E_{BSSE})$(kJ mol^{-1})	−40.3064(1.3158)	−43.0096 (3.6957)	−39.9409 (1.8142)
S2	$R(O_{CO}\cdots H_{H_2O})$, $\theta(O_{CO}\cdots HO_{H_2O})$	1.9395,161.45	1.9351,159.61	1.9372,161.44
	$R(H_{CH_3}\cdots O_{H_2O})$, $\theta(CH\cdots O_{H_2O})$	2.5505,137.09	2.5490,136.77	2.5477,136.99
	μ(debye)	1.9746	1.9446	1.9746
	$E(E_{ZP})$(hartree)	−305.567 735 12 (0.085 41)	−305.632 668 73 (0.085 35)	−305.654 745 89 (0.0855)
	$\Delta E(E_{BSSE})$(kJ mol^{-1})	−22.5694 (0.6428)	−24.4441 (1.5318)	−22.7452 (1.1392)
S3	$R(O_{OH}\cdots H_{H_2O})$, $\theta(O_{OH}\cdots HO_{H_2O})$	2.0806,157.80	2.0531,153.25	2.0726,157.06
	$R(H_{CH_3}\cdots O_{H_2O})$, $\theta(CH\cdots O_{H_2O})$	3.0037,103.31	2.5718,128.12	2.6832,125.61
	μ(debye)	1.8211	1.9843	1.7566
	$E(E_{ZP})$(hartree)	−305.563 767 60 (0.084 79)	−305.629 222 35 (0.085 18)	−305.650 929 87 (0.0851)
	$\Delta E(E_{BSSE})$(kJ mol^{-1})	−12.1527 (0.6514)	−15.3956 (1.8578)	−12.7262 (1.0435)
A1	$R(O_{CO}\cdots H_{H_2O})$, $\theta(O_{CO}\cdots HO_{H_2O})$	2.0066,179.83	2.0174,173.04	1.9977,179.84
	μ(debye)	7.008	7.4133	6.9981
	$E(E_{ZP})$(hartree)	−305.558 101 18 (0.085 07)	−305.622 000 88 (0.084 78)	−305.645 268 38 (0.0851)
	$\Delta E(E_{BSSE})$(kJ mol^{-1})	−19.1744 (0.6302)	−21.2118 (1.8889)	−19.2913 (1.0700)
A2	$R(O_{CO}\cdots H_{H_2O})$, $\theta(O_{CO}\cdots HO_{H_2O})$	1.9271,159.93	1.9381,156.86	1.9260,159.98
	$R(H_{CH_3}\cdots O_{H_2O})$, $\theta(CH\cdots O_{H_2O})$	2.4695,138.35	2.4436,138.60	2.4692,138.28
	μ(debye)	3.2913	3.1632	3.2843
	$E(E_{ZP})$(hartree)	−305.560 238 109 (0.085 39)	−305.624 150 89 (0.085 08)	−305.647 427 04 (0.085 48)
	$\Delta E(E_{BSSE})$(kJ mol^{-1})	−24.7849 (0.7298)	−26.8567 (1.6152)	−24.9588 (1.1391)
A3	$R(H_{OH}\cdots O_{H_2O})$, $\theta(OH\ldots O_{H_2O})$	1.8652,169.75	1.8549,170.65	1.8617,169.58
	μ(debye)	6.2632	6.8098	6.3954
	$E(E_{ZP})$(hartree)	−305.561 915 44 (0.085 31)	−305.626 882 40 (0.085 08)	−305.649 066 13 (0.085 28)
	$\Delta E(E_{BSSE})$(kJ mol^{-1})	−29.1888 (0.7511)	−34.0283 (4.2360)	−29.2623 (1.4874)

in the corresponding C═O bond length. Furthermore, the O–H bonds in acetic acid and in water that are directly involved in H bonding (with the dangling O in water and the carbonyl group in acetic acid, respectively) are also found to lengthen slightly. Of interest is the (nonstandard) modified basis set, 6-31+G(3d,p), optimized by Ochterski for modeling H-bonding interaction.[21,22] Table I clearly shows that while the corresponding total energy E differs the most from that obtained by the largest basis set, the corresponding binding energy ΔE obtained by the 6-31+G(3d,p) basis set (with 185 basis functions) is quite close to that provided by the largest basis set (with 303 basis functions). The Ochterski basis set is therefore only slightly larger than the 6-311++G(d,p) basis set (with 152 basis functions) but could provide ΔE values of similar quality to the much larger basis set. The use of such a basis set therefore offers considerable cost saving for computing properties of large, weakly bonded (hydrate) systems (involving H-bonding interactions).

Given that H bonding is commonly considered primarily as a weak electrostatic interaction in nature, it has been suggested that the H bonds in hydrates generally exhibit a bond length less than 2.4 Å and a bond angle greater than 120°,[31] with a bond energy of 10.5 kJ mol^{-1}.[32] We therefore consider the existence of a H bond when the bond length is less than 2.4 Å. Since the other two basis sets provide rather similar values for the properties, we focus our discussion only on the results obtained by the largest basis set, 6-311++G(3df,3pd). The binding energy obtained by the present calculation should be a good measure of the H-bonding interactions in the hydrates. Of the six conformer monohydrate structures shown in Fig. 1, the S1 conformer is found to be the most strongly bound structure, with ΔE (−39.9409 kJ mol^{-1}) nearly twice that of those for most other conformers. The S1 conformer is unique because it corresponds to a cyclic complex bound together by two H bonds: one between the carbonyl O and the dangling H_{H_2O} [with $R(O_{CO}\cdots H_{H_2O})=1.960$ Å and $\theta(O_{CO}\cdots HO_{H_2O})=139.82°$] and the second one between the hydroxyl H and the dangling O_{H_2O} [with $R(H_{OH}\cdots O_{H_2O})=1.8068$ Å and $\theta(OH\cdots O_{H_2O})=157.11°$] (Table II). (The subscript indicates the functional group of the acetic acid or the water molecule

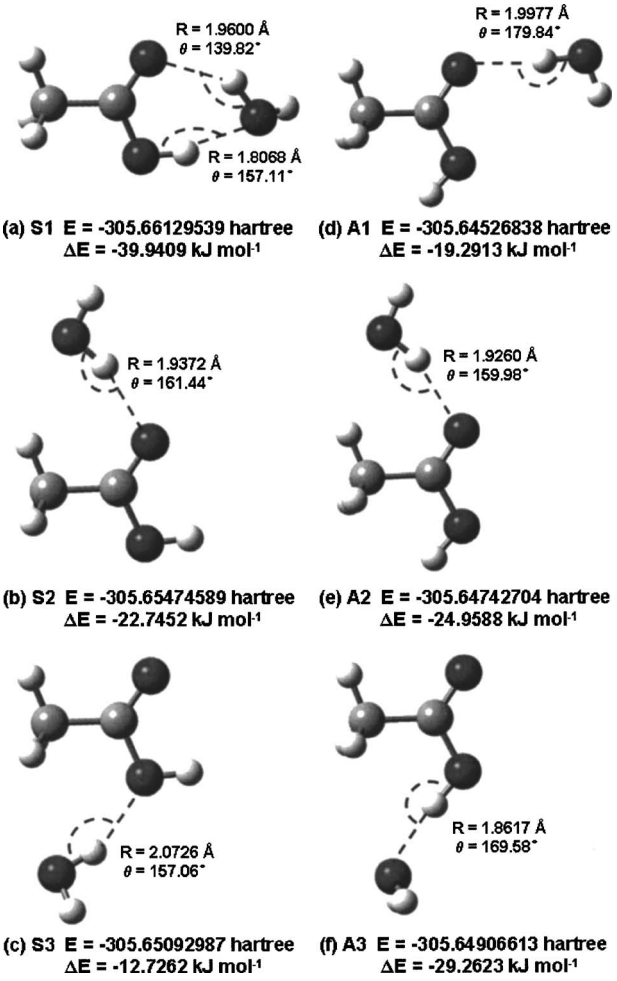

FIG. 1. Equilibrium structures and the corresponding total energies E and binding energies ΔE of the conformers of acetic acid monohydrate.

to which the atom belongs.) As shown in Fig. 1(a), the H atom in the water molecule not involved in the H bonding lies out of the molecular plane of the acetic acid. For the S2 and S3 conformers, only one H bond (with a longer bond length) is formed between the dangling H_{H_2O} and the carbonyl O [with $R(O_{CO}\cdots H_{H_2O})=1.9372$ Å and $\theta(O_{CO}\cdots HO_{H_2O})=161.44°$] and the hydroxyl O [with $R(O_{OH}\cdots H_{H_2O})=2.0726$ Å and $\theta(O_{OH}\cdots HO_{H_2O})=157.06°$], respectively [Figs. 1(b) and 1(c)]. The methyl group of the acetic acid in these conformers only provides rather weak interaction with the dangling O in water, giving a bond length $R(H_{CH_3}\cdots O_{H_2O})$ greater than 2.4 Å. Due to the nature of the *anti*-conformer structure of the acetic acid molecule itself, the A1–A3 monohydrate conformers [Figs. 1(d)–1(f)] can essentially be considered as resulting from the formation of one H bond. In particular, A1 involves the formation of a H bond between the carbonyl O and the dangling H_{H_2O} [with $R(O_{CO}\cdots H_{H_2O})=1.9977$ Å and $\theta(O_{CO}\cdots HO_{H_2O})=179.84°$]. The formation of a second H bond (as in S1) is not feasible due to the orientation of the hydroxyl group [Fig. 1(d)]. Similarly, A2 and A3 involve the formation of a H bond between the carbonyl O and the dangling H_{H_2O} [with $R(O_{CO}\cdots H_{H_2O})=1.926$ Å and $\theta(O_{CO}\cdots HO_{H_2O})=159.98°$] and that between the hydroxyl H and the dangling O_{H_2O} [with $R(H_{OH}\cdots O_{H_2O})=1.8617$ Å and $\theta(OH\cdots O_{H_2O})=169.58°$], respectively [Figs. 1(e) and 1(f)]. Based on the calculated bond lengths, we could infer the general strength associated with the different types of H bonding obtained for the S and A monohydrate conformers. In particular, the H bonding between the hydroxyl H and dangling O_{H_2O} [with $R(H_{OH}\cdots O_{H_2O})=1.8068$ Å (S1), 1.8617 Å (A3)] is stronger than that between the carbonyl O and dangling H_{H_2O} [with $R(O_{CO}\cdots H_{H_2O})=1.960$ Å (S1), 1.9372 Å (S2), 1.9977 Å (A1), 1.926 Å (A2)] and that between the hydroxyl O and dangling H_{H_2O} [with $R(O_{OH}\cdots H_{H_2O})=2.0726$ Å (S3)] (Table II). The observed relative bond strengths of these H-bonding types are consistent with the stronger electron donating nature of the carbonyl group than the hydroxyl group in acetic acid.

Table II also shows that the total energies (E) of the *anti*-monohydrate conformers (A1, A2, and A3) are generally less negative than their *syn*-counterparts (S1, S2, and S3), which is consistent with the less negative total energies of individual monohydrate conformers relative to the *syn*-conformer of the acetic acid molecule (shown in Table I). The relative stabilities for S2 (17.2 kJ mol^{-1}), S3 (27.2 kJ mol^{-1}), A1 (32.1 kJ mol^{-1}), A2 (36.4 kJ mol^{-1}), and A3 (42.1 kJ mol^{-1}) are considerably greater than 2.5 kJ mol^{-1}, indicating that the existence of these conformers is not thermodynamically viable at room temperature. On the other hand, the ΔE values follow the trend S1(−39.9409 kJ mol^{-1}) > A3(−29.2623 kJ mol^{-1}) > A2(−24.9588kJ mol^{-1}) > S2(−22.7452 kJ mol^{-1}) > A1 (−19.2913 kJ mol^{-1}) > S3(−12.7262 kJ mol^{-1}), which depends on the number and the types of H-bonding involved. This trend reflects how readily thermodynamically the monohydrate could be separated into the individual acetic acid and water molecules. It should be noted that since the presence of transition states has not been investigated in our calculations, our results could therefore only be used to evaluate the thermodynamical viability of the process. Evidently, the ΔE values of these conformers suggest that the bond strength of a H bond in the monohydrate is approximately 20 kJ mol^{-1} and is therefore considerably smaller than the bond enthalpy of a normal covalent bond (300–450 kJ mol^{-1}), i.e., 5%–10% of that of a covalent bond. The experimental binding enthalpy of water dimer has been reported to be 15±2 kJ mol^{-1} by Curtiss *et al.*,[33] in good accord with the DFT/6-311++G(3*df*,3*pd*) result obtained by us (17.2 kJ mol^{-1}). The present calculation shows that the binding energy of the most stable monohydrate conformer S1 is nearly twice of those of the calculated (and experimental) values of the water dimer, which supports the hypothesis of coevaporation of acetic acid and water upon annealing acetic acid adsorbed on an ultrathin ice film proposed in our recent work.[23]

Table III compares the vibrational wave numbers and IR intensities of the *syn*- and *anti*-conformers of acetic acid and the six acetic acid monohydrate conformers obtained by the B3LYP/6-311++G(3*df*,3*pd*) calculation with the corresponding gas-phase[34] and matrix experimental data.[35] Except for the COH bending mode δ(COH), most of the vibrational modes for the *syn*- and *anti*-conformers of acetic acid all

TABLE III. Comparison of the wave numbers (cm^{-1}) of fundamental vibrations of *syn*- and *anti*-acetic acid, acetic acid monohydrates and dihydrates obtained by DFT at the B3LYP/6−311++G(3*df*,3*pd*) level with the available experimental data. The relative intensities of the calculated vibrational modes are given in round parentheses.

	Assignment[a]	Gas[b,c]	Ar matrix[b,d]	*Syn*-acetic acid	Antiacetic acid	S1	S2	S3	A1	A2	A3
Acetic acid bands	ν(OH)	3583	3566	3754 (60)	3810 (46)	3394 (560)	3751 (62)	3752 (88)	3809 (55)	3809 (54)	3584 (622)
	$\nu_{s'}(CH_3)$	3051	⋯	3164 (4)	3158 (3)	3163 (6)	3168 (0.4)	3166 (3.1)	3161 (2)	3160 (2)	3156 (7)
	$\nu_{as}(CH_3)$	2996	⋯	3112 (3)	3095 (6)	3112 (3)	3112 (2)	3113 (1.6)	3098 (4)	3095 (4)	3100 (8)
	$\nu_s(CH_3)$	2944	⋯	3054 (2)	3038 (4)	3054 (1)	3054 (3)	3054 (0.8)	3040 (3)	3038 (9)	3043 (5)
	ν(C=O)	1788 (vs)	1779 (vs)	1820 (345)	1854 (303)	1772 (309)	1793 (387)	1832 (353)	1840 (359)	1828 (328)	1834 (333)
	$\delta_{as}(CH_3)$	1430	1439	1478 (8)	1488 (8)	1478 (8)	1480 (8)	1480 (12)	1488 (8)	1492 (7)	1487 (7)
	$\delta_{s'}(CH_3)$	1430	1434	1473 (16)	1473 (7)	1473 (25)	1475 (12)	1472 (19)	1472 (8)	1476 (3)	1470 (7)
	$\delta_s(CH_3)$	1382	1380 (*m*)	1409 (45)	1400 (41)	1449 (34)	1419 (51)	1414 (37)	1403 (42)	1410 (43)	1400 (55)
	δ(COH)	1264	1181 (vs)	1337 (35)	1200 (4)	1396 (23)	1350 (57)	1324 (28)	1211 (2)	1216 (2)	1249 (59)
	ν(C−O)	1182 (*s*)	1259 (*m*)	1203 (214)	1293 (388)	1292 (249)	1216 (207)	1202 (225)	1301 (371)	1306 (428)	1346 (400)
	$\rho_{\perp}(CH_3)$	1048	1044	1070 (7)	1064 (5)	1073 (8)	1076 (8)	1072 (8)	1068 (5)	1072 (6)	1065 (4)
	$\rho_{\parallel}(CH_3)$	989	987 (*s*)	1000 (76)	988 (12)	1022 (34)	1016 (70)	999 (90)	996 (8)	1008 (9)	1004 (14)
	ν(CC)	847	⋯	859 (4)	857 (31)	888 (13)	868 (3)	850 (10)	866 (28)	868 (24)	872 (17)
Water bands	ν_{as}(OH)	3734		3915 (60)		3875 (84)	3889 (86)	3894 (117)	3886 (84)	3889 (83)	3898 (92)
	ν_s(OH)	3638		3816 (4)		3617 (402)	3674 (377)	3765 (120)	3723 (342)	3663 (380)	3804 (16)
	δ(HOH)	1589		1626 (72)		1627 (121)	1649 (96)	1640 (64)	1654 (76)	1650 (100)	1632 (72)
	Assignment					S11	S12	S13	S22	S23	S33
Acetic acid bands	ν(OH)			3754 (60)		3146 (1101)	3360 (702)	3328 (759)	3750 (63)	3747 (76)	3750 (62)
	$\nu_{s'}(CH_3)$			3164 (4)		3162 (40)	3163 (1)	3164 (5)	3154 (15)	3166 (2)	3161 (4)
	$\nu_{as}(CH_3)$			3112 (3)		3112 (4)	3111 (2)	3111 (2)	3106 (2)	3110 (1)	3099 (14)
	$\nu_s(CH_3)$			3054 (2)		3054 (1)	3052 (2)	3051 (1)	3047 (12)	3050 (1)	3039 (20)
	ν(C=O)			1820 (345)		1751 (366)	1748 (343)	1785 (319)	1784 (431)	1805 (398)	1835 (355)
	$\delta_{as}(CH_3)$			1478 (8)		1479 (8)	1483 (8)	1481 (13)	1488 (7)	1485 (12)	1488 (13)
	$\delta_{s'}(CH_3)$			1473 (16)		1475 (17)	1476 (22)	1474 (23)	1479 (20)	1474 (13)	1476 (19)
	$\delta_s(CH_3)$			1409 (45)		1462 (23)	1457 (54)	1450 (18)	1422 (48)	1419 (40)	1420 (30)
	δ(COH)			1337 (35)		1397 (46)	1402 (21)	1405 (30)	1352 (60)	1337 (47)	1323 (20)
	ν(C−O)			1203 (214)		1312 (288)	1312 (248)	1282 (273)	1219 (200)	1217 (238)	1202 (240)
	$\rho_{\perp}(CH_3)$			1070 (7)		1073 (7)	1077 (9)	1075 (8)	1079 (8)	1079 (8)	1074 (7)
	$\rho_{\parallel}(CH_3)$			1000 (76)		1032 (25)	1036 (31)	1026 (42)	1013 (80)	1016 (86)	1000 (108)
	ν(CC)			859 (4)		893 (4)	896 (7)	882 (12)	872 (2)	861 (5)	846 (17)
Water bands	ν_{as}(OH)			3915 (60)		3876 (78) 3871 (74)	3886 (82) 3874 (99)	3890 (116) 3873 (90)	3882 (58) 3879 (92)	3895 (114) 3888 (105)	3882 (70) 3878 (119)
	ν_s(OH)			3816 (4)		3515 (960) 3408 (713)	3672 (187) 3657 (508)	3748 (200) 3633 (317)	3615 (585) 3563 (532)	3775 (100) 3692 (350)	3706 (332) 3621 (388)
	δ(HOH)			1626 (72)		1663 (73) 1645 (80)	1650 (68) 1621 (131)	1639 (40) 1625 (130)	1666 (36) 1649 (75)	1647 (78) 1631 (65)	1658 (24) 1645 (85)

[a] ν=stretch, δ=scissors, ρ=rock, γ=twist, *s*=symmetric, as=asymmetric.
[b] vs=very strong, *s*=strong, and *m*=medium
[c] Reference 34.
[d] Reference 35.

have very similar wave-number values (to within 2%). However, discernible differences are observed in the relative intensities of the vibrational modes between the two acetic acid conformers, reflecting the structural differences of these conformers. The calculated wave numbers of the more stable *syn*-acetic acid conformer differ from the observed wave numbers for both the gas-phase[34] and matrix data[35] by as much as 4.6% for ν(OH) in the high-wave-number end to 1.4% for ν(CC) in the other end. The relative intensities of the *syn*-acetic acid conformer are found to be in better accord with the experimental results[34] than the less stable *anti*-conformer.

In the case of the acetic acid monohydrate conformers, most of the wave numbers, particularly those involving the $C-CH_3$ backbone, are found to be similar to one another. However, notable differences are observed in the vibrational wave numbers of the bonds directly involved in H bonding. To illustrate the effects of H bonding with a water molecule in the monohydrate, we consider the wave-number shifts $\Delta\nu$ of the vibrations for the S1–S3 and the A1–*A*3 monohydrate conformers with respect to the *syn*- and *anti*-acetic acid conformers, respectively. In particular, the ν(C=O) stretching wave numbers for all the monohydrate conformers (Table III) are found to undergo a redshift (with respect to the re-

spective *syn*- or *anti*-acetic acid conformer) [$\Delta\nu=-48$ cm^{-1} (S1), -27 cm^{-1} (S2), -14 cm^{-1} (A1), -26 cm^{-1} (A2), and -20 cm^{-1} (A3)], with the exception of S3 ($\Delta\nu=+12$ cm^{-1}) where a blueshift is observed. On the other hand, the corresponding wave numbers for ν(C–O) [δ(COH)] for the monohydrate conformers all exhibit a blueshift [$\Delta\nu=+89$ cm^{-1}(+59 cm^{-1}) for S1, +13 cm^{-1}(+13 cm^{-1}) for S2, +8 cm^{-1}(+11 cm^{-1}) for A1, +13 cm^{-1}(+16 cm^{-1}) for A2, and +53 cm^{-1}(+49 cm^{-1}) for A3], with the exception of S3 [$\Delta\nu=-1$ cm^{-1} for ν(C–O) and -13 cm^{-1} for δ(COH)]. These C–O-related vibrational shifts therefore appear to be anticorrelated with the observed shift for the ν(C=O) mode. In the case of the ν(OH) stretching mode, the redshifts for S1 ($\Delta\nu=-360$ cm^{-1}) and A3 ($\Delta\nu=-226$ cm^{-1}) are considerably larger while the corresponding redshifts for other conformers [$\Delta\nu=-3$ cm^{-1} (S2), -2 cm^{-1} (S3), and -1 cm^{-1} (A1 and A2)] are near zero. The observed redshifts in ν(C=O) and ν(OH) for the acetic acid monohydrate conformers are consistent with the redshifts typically found in the vibrational wave numbers of bonds directly involved in H bonding for other H-bonded complexes.[28] Table III also shows that the wave numbers and intensities of the ν(CC) stretching and other vibrational modes involving the methyl group are only slightly affected by the presence of the water molecule, which is consistent with the equilibrium structure of the monohydrate that involves no direct interaction between that part of the acetic acid and the water molecule. For the vibrational modes of water in the monohydrate, notable redshifts are also observed in the ν_s(OH) symmetric stretching mode with respect to that of a free water molecule (Table III). The formation of H bonds in the monohydrate therefore weakens the adjacent covalent bonds in the constituent acetic acid and water molecules. The calculated changes in the vibrational wave numbers are generally consistent with the corresponding changes in the respective bond distances upon monohydrate formation, as observed above. It should be noted because the wave-number shifts $\Delta\nu$ are expected to be relatively insensitive to the different computational methods given a sufficiently large basis set, the present calculations for acetic acid monohydrate could therefore be used to predict the corresponding IR spectrum by combining with the measured spectra of the corresponding constituent molecules.

In addition, there is generally no significant change in the calculated intensities of most of the vibrational modes of the acetic acid monohydrates from those of their respective *syn*- and *anti*-acetic acid conformers, except for the ν(OH) of the acetic acid band for S1 and A3 and ν_s(OH) of the water band for S1, S2, S3, A1, and A2. These changes in the OH stretching bands are expected because of the increased sharing of the H atoms in the respective OH bonds upon monohydrate formation. In particular, the enhanced H sharing is clearly evident from the equilibrium structures of the S1 and A3 conformers [Fig. 1], where the hydroxyl group of the acetic acid molecule is in effect partially "donating" the H atom to the dangling O atom of the water molecule in the formation of the monohydrate. Similarly, the water molecule is partially donating its H atom to the carbonyl group of the acetic acid in the S1, S2, A1, and A2 monohydrate conformers and to the hydroxyl group of the acetic acid in S3 (Fig. 1). In summary, the formation of H bonds reduces the force constants of the adjacent (covalent) bonds in the constituent molecules, causing the redshifts in the corresponding vibrational (stretching) modes. The increased sharing of the H atoms as a result of the H-bond formation increases the dipole moments of the adjacent bonds and correspondingly the spectral intensities of the respective vibrational modes.

B. Conformers of acetic acid dihydrate

We have also determined the equilibrium structures for the six conformers of the acetic acid dihydrate by using DFT-B3LYP calculations with the nonstandard 6-31+G($3d,p$) and the standard 6-311++G(d,p) and 6-311++G($3df,3pd$) basis sets, with 226, 188, and 378 basis functions, respectively. Selected structural parameters along with the dipole moment, the total energy E without the E_{ZP} correction, and the binding energy ΔE without the E_{BSSE} correction obtained by these calculations are presented in Table IV. As with the earlier calculations for the monohydrate conformers, the structural parameters and the energies obtained for these basis sets are very similar to one another for all of the conformers. The basis set 6-31+G($3d,p$) by Ochterski[22] (with the least negative total energy E) provides ΔE values and dipole moments similar to those obtained by the largest basis set but with a considerably smaller number of basis functions. The conformer structures obtained by the largest basis set, 6-311++G($3df,3pd$), are also energetically most stable (i.e., with the most negative total energies), and they are shown in Fig. 2.

Table IV shows that the total energy of S11 is the most negative ($E=-382.143\,412\,99$ hartree), while the relative stabilities of the other conformers follow the trend S11 > S12(24.4 kJ mol^{-1}) > S13(31.3 kJ mol^{-1}) > S22(31.4 kJ mol^{-1}) > S33(45.4 kJ mol^{-1}) > S23(52.3 kJ mol^{-1}). Based on these relative stability data, the dihydrate is therefore primarily dominated by the S11 conformer. The ΔE values follow the same trend S11(-86.1657 kJ mol^{-1}) > S12(-61.8006 kJ mol^{-1}) > S13(-54.8455 kJ mol^{-1}) > S22 (-54.7112 mol^{-1}) > S33(-40.7231 kJ mol^{-1}) > S23(-33.8533 kJ mol^{-1}), which depends on the number and the nature of H bonding involved as discussed below. Table IV also shows that the ΔE value (-66.5338 kJ mol^{-1}) obtained for a cyclic acetic acid dimer is evidently more negative than those of all dihydrate conformers except for S11 [Fig. 2]. If we include the binding energy of a water dimer (-17.2 kJ mol^{-1}) to the ΔE value of the acetic acid dimer to account for the additional H bond (within the water dimer) in the S11 dihydrate conformer, the resulting ΔE value (-83.7 kJ mol^{-1}) is found to be remarkably similar to the S11 value (-86.1657 kJ mol^{-1}), which suggests that the H-bonding interactions between an acetic acid molecule and the two water molecules in the dihydrates are very similar indeed to those between two acetic acids.

As reflected by the ΔE values, the H-bonding interactions in the dihydrate conformers are found to be generally stronger than the monohydrate conformers, which indicate the presence of a greater number of H bonds with enhanced

TABLE IV. Comparison of the bond lengths R(Å) and bond angles θ(°), dipole moments μ, total energies E without the zero-point vibrational energy E_{ZP} corrections, and binding energies ΔE without the basis set superposition error E_{BSSE} corrections of the optimized equilibrium structures of acetic acid dihydrates and acetic acid dimer obtained by different calculations.

	Properties	DFT/6-31+G($3d,p$)	DFT/6-311++G(d,p)	DFT/6-311++G($3df,3pd$)
S11	$R(H_{OH}\cdots O_{H_2O})$, $\theta(OH\cdots O_{H_2O})$	1.6755, 175.88	1.6863, 177.69	1.6829, 176.80
	$R(O_{CO}\cdots H_{H_2O})$, $\theta(O_{CO}\cdots HO_{H_2O})$	1.7954, 167.63	1.8139, 164.57	1.7906, 167.42
	$R(H_{H_2O}\cdots O_{H_2O})$, $\theta(OH_{H_2O}\cdots O_{H_2O})$	1.7486, 161.34	1.7577, 158.72	1.7515, 160.91
	μ(debye)	0.4539	0.1907	0.4127
	$E(E_{ZP})$(hartree)	−382.032 216 67 (0.111 85)	−382.117 642 29 (0.111 93)	−382.143 412 99 (0.112 01)
	$\Delta E(E_{BSSE})$(kJ mole^{-1})	−85.3960 (2.3108)	−93.8696 (7.8405)	−86.1657 (2.9662)
S12	$R(H_{OH}\cdots O_{H_2O})$, $\theta(OH\cdots O_{H_2O})$	1.7767, 159.35	1.7790, 158.18	1.7819, 158.78
	$R(O_{CO}\cdots H_{H_2O})$, $\theta(O_{CO}\cdots HO_{H_2O})$	2.0147, 136.30	2.0419, 131.98	2.0183, 135.83
	$R(O_{CO}\cdots H_{H_2O})$, $\theta(O_{CO}\cdots HO_{H_2O})$	1.9336, 165.60	1.9235, 162.92	1.9285, 165.89
	$R(H_{CH_3}\cdots O_{H_2O})$, $\theta(CH\cdots O_{H_2O})$	2.6221, 136.51	2.5605, 137.12	2.6333, 136.34
	μ(debye)	1.6398	1.9601	1.6940
	$E(E_{ZP})$(hartree)	−382.023 267 04 (0.110 77)	−382.107 512 06 (0.110 74)	−382.134 132 79 (0.110 81)
	$\Delta E(E_{BSSE})$(kJ mole^{-1})	−61.8988(1.9807)	−67.2727 (5.9693)	−61.8006 (10.2946)
S13	$R(H_{OH}\cdots O_{H_2O})$, $\theta(OH\cdots O_{H_2O})$	1.7588, 158.98	1.7690, 158.13	1.7660, 158.55
	$R(O_{CO}\cdots H_{H_2O})$, $\theta(O_{CO}\cdots HO_{H_2O})$	1.9819, 137.58	2.0252, 132.91	1.9896, 136.96
	$R(O_{OH}\cdots H_{H_2O})$, $\theta(O_{OH}\cdots HO_{H_2O})$	2.0318, 161.98	2.0054, 158.24	2.0219, 162.32
	$R(H_{CH_3}\cdots O_{H_2O})$, $\theta(CH\cdots O_{H_2O})$	2.7900, 130.22	2.6390, 133.02	2.7763, 129.77
	μ(debye)	0.7691	1.3349	0.8318
	$E(E_{ZP})$(hartree)	−382.020 535 04 (0.110 36)	−382.104 989 23 (0.110 45)	−382.131 483 75 (0.110 47)
	$\Delta E(E_{BSSE})$(kJ mole^{-1})	−54.7259 (1.8016)	−60.6490 (2.6427)	−54.8455 (9.8911)
S22	$R(O_{CO}\cdots H_{H_2O})$, $\theta(O_{CO}\cdots HO_{H_2O})$	1.8546, 180.00	1.8589, 172.62	1.8499, 174.61
	$R(H_{CH_3}\cdots O_{H_2O})$, $\theta(CH\cdots O_{H_2O})$	2.3804, 173.27	2.3102, 175.01	2.3798, 176.10
	$R(H_{H_2O}\cdots O_{H_2O})$, $\theta(OH_{H_2O}\cdots O_{H_2O})$	1.8503, 165.17	1.8437, 164.18	1.8487, 167.26
	μ(debye)	1.9468	1.8396	1.9803
	$E(E_{ZP})$(hartree)	−382.020 149 03 (0.110 66)	−382.105 254 10 (0.110 92)	−382.131 432 61 (0.110 79)
	$\Delta E(E_{BSSE})$(kJ mole^{-1})	−53.7124 (1.4397)	−61.3445 (5.6517)	−54.7112 (8.8586)
S23	$R(O_{OH}\cdots H_{H_2O})$, $\theta(O_{OH}\cdots HO_{H_2O})$	2.1111, 154.83	2.0761, 151.22	2.0915, 155.55
	$R(H_{CH_3}\cdots O_{H_2O})$, $\theta(CH\cdots O_{H_2O})$	2.6998, 134.09	2.5770, 134.86	2.6917, 133.65
	$R(O_{CO}\cdots H_{H_2O})$, $\theta(O_{CO}\cdots HO_{H_2O})$	1.9590, 161.34	1.9623, 158.19	1.9561, 161.61
	$R(H_{CH_3}\cdots O_{H_2O})$, $\theta(CH\cdots O_{H_2O})$	2.5923, 135.28	2.5513, 135.57	2.6087, 135.15
	μ(debye)	2.8962	3.1605	2.9205
	$E(E_{ZP})$(hartree)	−382.012 364 12 (0.109 09)	−382.096 396 13 (0.109 28)	−382.123 488 23 (0.109 25)
	$\Delta E(E_{BSSE})$(kJ mole^{-1})	−33.2732 (1.0921)	−38.0879 (3.6296)	−33.8533 (1.3000)
S33	$R(O_{OH}\cdots H_{H_2O})$, $\theta(O_{OH}\cdots HO_{H_2O})$	2.0031, 172.59	1.9675, 169.43	1.9787, 171.54
	$R(H_{CH_3}\cdots O_{H_2O})$, $\theta(CH\cdots O_{H_2O})$	2.3818, 166.08	2.3123, 162.56	2.3974, 163.51
	$R(H_{H_2O}\cdots O_{H_2O})$, $\theta(OH_{H_2O}\cdots O_{H_2O})$	1.8955, 164.53	1.8801, 161.58	1.8903, 165.38
	μ(debye)	2.3288	2.8755	2.5292
	$E(E_{ZP})$(hartree)	−382.014 840 65 (0.110 06)	−382.100 287 49 (0.110 46)	−382.126 104 80 (0.110 22)
	$\Delta E(E_{BSSE})$(kJ mole^{-1})	−39.7753 (1.2220)	−48.3046 (5.8928)	−40.7231 (8.8194)
Acetic Acid Dimer	$R(H_{OH}\cdots O_{CO})$, $\theta(OH\cdots O_{CO})$	1.6458, 178.62	1.6835, 178.73	1.6561, 179.66
	μ(debye)	0.0010	0.0007	0.0007
	$E(E_{ZP})$(hartree)	−458.262 416 20 (0.125 15)	−458.354 609 01 (0.125 22)	−458.388 483 78 (0.1254)
	$\Delta E(E_{BSSE})$(kJ mole^{-1})	−66.2750 (2.2602)	−65.5158 (3.1402)	−66.5338 (−12.4194)

bond strengths in some cases. In particular, the ΔE value of the most stable dihydrate conformer S11 (−86.1657 kJ mol^{-1}) differs from that of the most stable monohydrate S1 (−39.9409 kJ mol^{-1}) by 46.2248 kJ mol^{-1}. Even after removing the contribution of the binding energy from a water dimer (with a typical ΔE of −17.2 kJ mol^{-1}), there remains a large difference of 29.0 kJ mol^{-1}, which clearly indicates that the H bonds formed between a water dimer and an acetic acid molecule are considerably stronger. Unlike a single water molecule in the monohydrate [Fig. 1(a)], the water dimer provides a more compatible structure to form collinear H bonds between O_{CO} with the dangling H of the water dimer and between H_{OH} with the dangling O of the water dimer in the dihydrate case [Fig. 2(a)]. The forma-

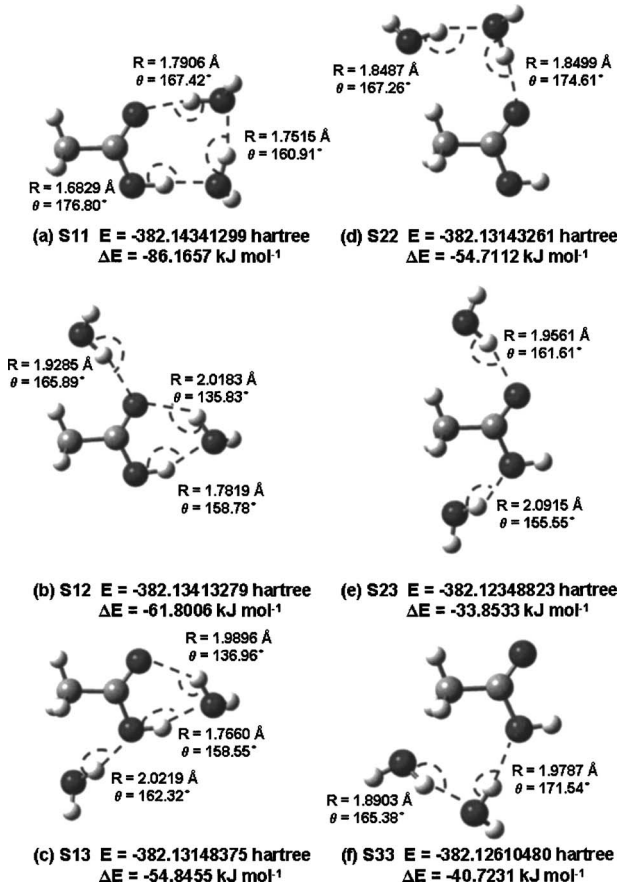

FIG. 2. Equilibrium structures and the corresponding total energies E and binding energies ΔE of the conformers of acetic acid dihydrate.

tion of a larger eight-member ring structure in the S11 dihydrate conformer [Fig. 2(a)], in contrast with the six-member ring structure in the S1 monohydrate conformer [Fig. 1(a)], therefore appears to have the effects of relieving the strain in all three H bonds. Similarly, enhanced H-bonding interactions between an acetic acid molecule and a water dimer are also found in the dihydrate conformers S22 [with $\Delta E = -54.7112$ kJ mol^{-1}, Fig. 2(d)] and S33 [with $\Delta E = -40.7231$ kJ mol^{-1}, Fig. 2(f)] with respect to the respective monohydrate conformers S2 [with $\Delta E = -22.7452$ kJ mol^{-1}, Fig. 1(b)] and S3 [with $\Delta E = -12.7262$ kJ mol^{-1}, Fig. 1(c)] after appropriate consideration of the ΔE value of a water dimer. In addition to the more open ring structures in these dihydrate conformers that relieve the H-bond strain, the dangling H atom in a water dimer could also be more reactive than that of a water monomer. In comparison with the respective monohydrate conformers, the dangling H atom of the water dimer evidently forms a shorter and more collinear H bond in the dihydrate conformers. In particular, the bond lengths and bond angles $R(O_{CO}\cdots H_{H_2O}) = 1.7906$ Å and $\theta(O_{CO}\cdots HO_{H_2O}) = 167.42°$ for S11, $R(O_{CO}\cdots H_{H_2O}) = 1.8499$ Å and $\theta(O_{CO}\cdots HO_{H_2O}) = 174.61°$ for S22, and $R(O_{OH}\cdots H_{H_2O}) = 1.9787$ Å and $\theta(O_{OH}\cdots HO_{H_2O}) = 171.54°$ for S33 are 0.1694, 0.0873, and 0.0939 Å shorter and 27.6°, 13.17°, and 14.48° larger than the corresponding H-bond lengths and angles in S1, S2, and S3, respectively. In the case of S11, the dangling O atom in the water dimer appears to form a stronger/shorter and more collinear H bond with the hydroxyl H of acetic acid {with $R(H_{OH}\cdots O_{H_2O}) = 1.6829$ Å and $\theta(OH_{OH}\cdots O_{H_2O}) = 176.80°$ [Fig. 2(a)]} than the corresponding H bond in S1 [with $R(H_{OH}\cdots O_{H_2O}) = 1.8068$ Å and $\theta(OH_{OH}\cdots O_{H_2O}) = 157.11°$] [Fig. 1(a)]. It should be noted that the H bond of the water dimer itself in the S11 dihydrate conformer is found to be shorter (1.7515 Å) and less collinear (160.91°) than those in S22 (1.8487 Å, 167.26°) and S33 (1.8903 Å. 165.38°), which could be the result of the formation of the stable eight-member ring structure in the S11 conformer.

The remaining dihydrate conformer structures do not involve the formation of a water dimer and the corresponding ΔE values may therefore be considered as the sum of the ΔE values of the contributing monohydrate conformers. In particular, the S12 [with $\Delta E = -61.8006$ kJ mol^{-1}, Fig. 2(b)] and S13 [with $\Delta E = -54.8455$ kJ mol^{-1}, Fig. 2(c)] dihydrate conformers may be regarded as a combination of the most stable S1 monohydrate structure [with $\Delta E = -39.9409$ kJ mol^{-1}, Fig. 1(b)] with S2 [with $\Delta E = -22.7452$ kJ mol^{-1}, Fig. 1(b)] and with S3 [with $\Delta E = -12.7262$ kJ mol^{-1}, Fig. 1(c)] respectively, while the S23 dihydrate conformer [with $\Delta E = -33.8533$ kJ mol^{-1}, Fig. 2(e)] can be regarded as a combination of S2 with S3. Unlike the conformers involving the water dimer (S11, S22, and S33), the energy differences between the ΔE values of the S12, S13, and S23 dihydrate conformers and the corresponding sums of the ΔE values of the contributing monohydrate conformers are considerably smaller (less than 2.2 kJ mol^{-1}), confirming the lack of any effective (correlated or collective) interaction between the two water molecules. Like the monohydrate conformers (Fig. 1), different types of H bonding (with different bond strengths) observed in the S12, S13, and S23 dihydrate conformers can also be categorized based on the corresponding bond lengths. In particular, the H bonding between the hydroxyl H and dangling O_{H_2O} [with $R(H_{OH}\cdots O_{H_2O}) = 1.7819$ Å (S12), 1.7660 Å (S13)] is stronger than that between carbonyl O and dangling H_{H_2O} [with $R(O_{CO}\cdots H_{H_2O}) = 1.9285$ Å and 2.0183 Å (S12), 1.9896 Å (S13), and 1.9561 Å (S23)] and that between hydroxyl O and dangling H_{H_2O} [with $R(O_{OH}\cdots H_{H_2O}) = 2.0219$ Å (S13) and 2.0915 Å (S23)] (Fig. 2, Table IV). The relative bond strengths of these H-bonding types observed in both monohydrate and dihydrate conformers are therefore consistent with the stronger electron donating nature of the carbonyl group than the hydroxyl group in acetic acid.

Except for the S11 conformer, the methyl H atoms in acetic acid in all other dihydrate conformers could interact with the dangling O in the water molecules. As shown in Table IV, these interactions are considerably weaker than the aforementioned H-bond interactions, giving a bond length $R(H_{CH_3}\cdots O_{H_2O})$ near 2.4 Å for S22 and S33 and above 2.6 Å for S12, S13, and S23. The discernibly shorter $R(H_{CH_3}\cdots O_{H_2O})$ bond lengths for S22 and S33 are likely due to the effects of H bonding in the water dimers of these conformers, which impose a less flexible structure.

Table III also shows the vibrational wave numbers and IR intensities of the six *syn*-acetic acid dihydrate conformers

obtained by the B3LYP/6-311++G($3df$,$3pd$) calculation. These results are compared with those calculated for *syn*-acetic acid and the monohydrate conformers S1, S2, and S3. Evidently, most of the wave numbers, particularly those involving the C–CH_3 backbone, are found to be similar to one another and to those found for the *syn*-acetic acid and the monohydrate conformers S1, S2, and S3. Like the monohydrates, discernible differences are observed in the more intense vibrational modes of the functional groups that are directly involved in H bonding. In particular, the ν(C═O) stretching wave numbers for most of the dihydrate conformers (Table III) are found to undergo a redshift (with respect to the respective *syn*-acetic acid conformer) [$\Delta\nu$=−69 cm^{-1} (S11), −72 cm^{-1} (S12), −35 cm^{-1} (S13), −36 cm^{-1} (S22), and −15 cm^{-1} (S23)], except for S33 ($\Delta\nu$=+15 cm^{-1}) that exhibits a blueshift. Interaction with the water dimer as in the dihydrate conformers S11, S22, and S33 therefore appears to increase the ν(C═O) wave-number shifts of the respective monohydrate conformers S1 ($\Delta\nu$=−48 cm^{-1}), S2 ($\Delta\nu$=−27 cm^{-1}), and S3 ($\Delta\nu$=+12 cm^{-1}), which confirms our earlier hypothesis that the dangling H of the water dimer is more reactive. Moreover, as with the corresponding wave-number shifts for ν(C-O) [δ(COH)] in the monohydrate conformers S1 [$\Delta\nu$=+89 cm^{-1} (+59 cm^{-1})] and S2 [$\Delta\nu$=+13 cm^{-1} (+12 cm^{-1})] that are anticorrelated with the ν(C═O) wave-number shifts, most of the dihydrate conformers also exhibit a blueshift for the ν(C–O) [δ(COH)] mode [$\Delta\nu$=+109 cm^{-1} (+60 cm^{-1}) for S11, +109 cm^{-1} (+65 cm^{-1}) for S12, +79 cm^{-1} (+68 cm^{-1}) for S13, +16 cm^{-1} (+15 cm^{-1}) for S22, and +14 cm^{-1} (0 cm^{-1}) for *S23*]. The minor redshift for the ν(C–O) [δ(COH)] mode observed for S33 [$\Delta\nu$=−1 cm^{-1} (−14 cm^{-1})] is found to be essentially identical to that of the S3 monohydrate conformer [$\Delta\nu$=−1 cm^{-1} (−13 cm^{-1})], which is not surprising given the similarities of the local structures of S33 and S3 at the hydroxyl group. Despite the secondary effects on the ν(C–O) [δ(COH)] shifts, the dangling H of the water dimer in the dihydrate conformers S11, S22, and S33 also appears to generally amplify these shifts. As expected from the similarities of the structures of the S13 [Fig. 2(c)] and S23 [Fig. 2(e)] conformers to their respective constituent monohydrate structures, these conformers exhibit ν(C═O) and ν(C–O) [δ(COH)] wave-number shifts common to those found in the S1 and S3 and in the S2 and S3 monohydrate conformers, respectively. For the S12 conformer, the effects of the second water molecule on the S1 conformer are more complex because of the bonding of the second water molecule to the carbonyl O [Fig. 2(b)]. In the case of the ν(OH) stretching mode, the redshift for S11 ($\Delta\nu$=−608 cm^{-1}) is found to be considerably larger than that for the monohydrate S1 ($\Delta\nu$=−360 cm^{-1}), which further confirms the enhanced bonding interactions in the eight-member ring structure. The ν(OH) redshifts for S12 ($\Delta\nu$=−394 cm^{-1}) and S13 ($\Delta\nu$=−426 cm^{-1}) are larger than that of S1, reflecting the effects exerted by the second water molecule on the carbonyl group in S12 and on the hydroxyl group in S13, respectively. As expected from the near-zero shifts in ν(OH) for the monohydrate conformers S2 ($\Delta\nu$=−3 cm^{-1}) and S3 ($\Delta\nu$=−2 cm^{-1}), and the corresponding redshifts for other dihydrate conformers [$\Delta\nu$=−4 cm^{-1} (S22), −7 cm^{-1} (S23), −4 cm^{-1} (S33)] are almost close to zero, which again illustrates the minimal effects of the water molecules to the local OH bond in these dihydrate conformers.

The vibrational modes of water in the dihydrate conformers S12, S13, and S23 can generally be considered similar to those found in their contributing constituent monohydrate conformers S1, S2, and S3. For the dihydrate conformers with the water dimer, S11, S22, and S33, there appear to be larger redshifts in the ν_s(OH) symmetric stretching mode from that of a free water molecule with respect to the S1, S2, and S3 monohydrate conformers, respectively, (Table III). Like the monohydrates, the formation of H bonds in these dihydrate conformers therefore generally weakens the adjacent covalent bonds in the constituent acetic acid and water molecules. The calculated changes in the vibrational wave numbers are generally consistent with the corresponding changes in the respective bond lengths upon hydrate formation, and the evolution of the calculated wave-number shifts $\Delta\nu$ from monohydrates to dihydrates could be useful to infer experimental spectrum of acetic acid adsorbed on an ultrathin ice film.[23]

The calculated intensities of most of the vibrational modes of the acetic acid dihydrate conformers follow those of the contributing monohydrate conformers. In particular, the calculated spectra of S22 and S33 closely resemble those of S2 and S3, respectively, while that for S23 may be regarded as a combination of those of S2 and S3 (Table III). In the case of S11, S12, and S13, the calculated spectral intensities are generally similar to those of S1, with the exception of the ν(OH) band for acetic acid, which is considerably more intense in the dihydrate conformers than that found in S1. The near doubling in the ν(OH) spectral intensity for the S11 dihydrate conformer with respect to the S1 conformer is correlated with the reduction in the H-bond length $R(H_{OH}\cdots O_{H_2O})$ by 0.1239 Å from that of S1 due to the formation of the eight-member ring structure [Fig. 2(a)]. Similarly, the increases in the ν(OH) spectral intensities for the S12 and S13 dihydrate conformers by at least 25% are related to the less pronounced bond shortening in the $R(H_{OH}\cdots O_{H_2O})$ from that for S1 {0.0249 Å for S12 [Fig. 2(b)] and 0.0408 Å for S13 [Fig. 2(c)]}, which are related to the more subtle intramolecular structural changes to the acetic acid as a result of the addition of the second water molecule. These structural changes affect the extent that the hydroxyl group of the acetic acid molecule is donating the H atom to the dangling O atom of the water molecule in the formation of the dihydrate. Similarly, the water molecule is partially donating its H atom to the carbonyl group of the acetic acid in the S1, S2, A1, and A2 monohydrate conformers and to the hydroxyl group of the acetic acid in S3 (Fig. 1). In summary, the formation of H bonds reduces the force constants of the adjacent (covalent) bonds in the constituent molecules, causing the redshifts in the corresponding vibrational (stretching) modes. The increased sharing of the H atoms as a result of the H-bond formation increases the dipole moments of the adjacent bonds and correspondingly the spectral intensities of these vibrational modes.

IV. CONCLUDING REMARKS

The H-bonding interactions in acetic acid monohydrates and dihydrates have been studied by using DFT calculations with different basis sets. The nonstandard diffuse polarization basis set, 6-31+G($3d,p$), can be used to provide relatively accurate results with considerably lower computational cost. We obtain the structures and energetics of six monohydrate conformers (three with *syn*-acetic acid and three with *anti*-acetic acid) and six dihydrate conformers with *syn*-acetic acid, of which the respective cyclic double-H-bonded structures S1 and S11 are found to be the most stable. Evidently, the binding energies of monohydrates and dihydrates follow the trends $S1>A3>A2>S2>A1>S3$ and $S11>S12>S13>S22>S33>S23$, respectively. The binding energies (per hydrogen bond) of the most stable monohydrate and dihydrate conformers (S1 and S11) are also found to be discernibly larger than that of the water dimer. This result supports our recent FTIR-RAS observation of coevaporation of acetic acid and water upon annealing acetic acid on ice.[23] The calculated vibrational wave numbers and intensities of monohydrates and dihydrates are found to be generally consistent with the reported experimental gas-phase and matrix data[34,35] and can be understood in terms of spectral evolution as a result of hydrate formation.

ACKNOWLEDGMENT

This work was supported by the Natural Sciences and Engineering Research Council of Canada.

[1] C. Girardet and C. Toubin, Surf. Sci. Rep. **44**, 159 (2001).
[2] P. Pulay, Mol. Phys. **21**, 329 (1971).
[3] H. B. Schlegel, S. Wolfe, and F. Bernardi, J. Chem. Phys. **63**, 3632 (1975).
[4] C. E. Blom and C. Altona, Mol. Phys. **31**, 1377 (1976).
[5] A. Burneau, F. Génin, and F. Quilès, Phys. Chem. Chem. Phys. **2**, 5020 (2000).
[6] J. B. Foresman and Æ. Frisch, *Exploring Chemistry with Electronic Structure Methods* (Gaussian Inc., Pittsburgh, 1996).
[7] C. Seife, Science **274**, 2012 (1996).
[8] D. R. Haynes, N. J. Tro, and S. M. George, J. Phys. Chem. **96**, 8502 (1992).
[9] D. E. Brown and S. M. George, J. Phys. Chem. **100**, 15460 (1996).
[10] C. Toubin, P. N. M. Hoang, S. Picaud, and C. Girardet, Chem. Phys. Lett. **329**, 331 (2000).
[11] J. J. Novoa and M. H. Whangbo, J. Am. Chem. Soc. **113**, 9017 (1991).
[12] A. D. Becke, J. Chem. Phys. **97**, 9173 (1992).
[13] A. D. Becke, J. Chem. Phys. **98**, 5648 (1993).
[14] C. Lee, W. Yang, and R. G. Parr, Phys. Rev. B **37**, 785 (1988).
[15] Z. Latajka and Y. J. Bouteiller, J. Chem. Phys. **101**, 9793 (1994).
[16] K. Kim and K. D. Jordan, J. Phys. Chem. **98**, 10089 (1994).
[17] J. E. Del Bene, W. B. Person, and K. J. Szczepaniak, J. Phys. Chem. **99**, 10705 (1995).
[18] J. Florián and B. G. Johnson, J. Phys. Chem. **98**, 3681 (1994).
[19] P. J. Stephens, F. J. Devlin, C. F. Chabalowski, and M. J. Frisch, J. Phys. Chem. **98**, 11623 (1994).
[20] J. Wang, L. A. Eriksson, R. J. Boyd, Z. Shi, and B. G. Johnson, J. Phys. Chem. **98**, 1844 (1994).
[21] P. R. Rablen, J. W. Lockman, and W. L. Jorgensen, J. Phys. Chem. A **102**, 3782 (1998).
[22] J. W. Ochterski, Ph.D. thesis, Wesleyan University, 1994.
[23] Q. Gao and K. T. Leung, J. Phys. Chem. B (in press).
[24] Gaussian 98 (Revision A.11.3), M. J. Frisch, G. W. Trucks, H. B. Schlegel *et al.*, Gaussian Inc., Pittsburgh, PA, 2002.
[25] F. B. Vanduijneveldt, J. G. C. M. Van Duijneveldt-Vande Rijdt, and J. H. Van Lenthe, Chem. Rev. (Washington, D.C.) **94**, 1873 (1994).
[26] S. F. Boys and F. Bernardi, Mol. Phys. **19**, 553 (1970).
[27] P. Valiron and I. Mayer, Chem. Phys. Lett. **275**, 46 (1997).
[28] Z. Y. Zhou, Y. Shi, and X. M. Zhou, J. Phys. Chem. A **108**, 813 (2004).
[29] H. Sato and F. Hirata, J. Mol. Struct.: THEOCHEM **461–462**, 113 (1999).
[30] J. L. Derissen, J. Mol. Struct. **7**, 67 (1971).
[31] C. Molteni and M. Parrinello, J. Am. Chem. Soc. **120**, 2168 (1998).
[32] G. G. Malenkov, D. L. Tytik, and E. A. Zheligovskaya, J. Mol. Liq. **82**, 27 (1999).
[33] L. A. Curtiss, D. J. Frurip, and M. J. Blander, J. Chem. Phys. **71**, 2703 (1979).
[34] M. Haurie and A. Novak, J. Chim. Phys. Phys.-Chim. Biol. **62**, 137 (1965).
[35] C. V. Berney, R. L. Redington, and K. C. Lin, J. Chem. Phys. **53**, 1713 (1970).